Absorption spectra and Zeeman effect of the trivalent holmium ion in compounds with tetragonal zircon structure. I. Ho^{3+} in YVO_4

1990 J. Phys.: Condens. Matter 2 4685

(http://iopscience.iop.org/0953-8984/2/21/003)

J. Phys.: Condens. Matter **2** (1990) 4685–4700. Printed in the UK

Absorption spectra and Zeeman effect of the trivalent holmium ion in compounds with tetragonal zircon structure: I. Ho^{3+} in YVO_4

M Enderle†, B Pilawa, W Schlaphof‡ and H G Kahle
Physikalisches Institut, Universität Karlsruhe (TH), POB 6980, D-7500 Karlsruhe 1, Federal Republic of Germany

Received 6 December 1989

Abstract. The optical absorption spectrum of Ho^{3+} in tetragonal $(Ho_{0.1},Y_{0.9})VO_4$ was studied in the range from 11 000 to 27 600 cm^{-1} at temperatures between 1.4 and 85 K in magnetic fields up to 4 T. Fields along the crystal *c* axis were used to determine the splitting factors of the doublets. Fields perpendicular to *c* were applied to induce transitions from the lowest singlet of the ground term, which are forbidden without the field. The energies and the symmetry types of almost all crystal-field components could be established with great certainty.

1. Introduction

The optical spectra of crystalline compounds of trivalent holmium have been of interest for a long time. The first investigations on the chloride hexahydrate (Kahle 1956) and the ethyl sulphate (Grohmann *et al* 1961, Hüfner 1962) were mainly concerned with the determination of the terms of Ho^{3+} that take part in the optical transitions; particulars of the crystal-field splittings, however, were already included. Extensive studies on Ho^{3+} in anhydrous $LaCl_3$ were initiated by the group at Johns Hopkins University, Baltimore, USA (Crosswhite *et al* 1977, Rajnak and Krupke 1967). Investigations on Ho^{3+} in YPO_4, encompassing calculations on crystal-field splittings and line intensities, were published by former members of our group (Becker *et al* 1969, Becker 1970, 1971).

All these substances have in common that the description of the experimentally observed crystal-field splittings of the Ho^{3+} ion by means of calculations in a one-ion model with independent 4f electrons leads to very unsatisfactory results (Becker 1970, Domann 1974, Rajnak and Krupke 1967). It is possible to minimise the deviations between experimental and theoretical results for some of the terms in question (e.g. for the ^5F terms), but as a consequence the deviations become exceptionally large for the remaining terms (e.g. for $^3K_8$ and $^5G_6$). These discrepancies caused Judd (1977) to introduce the spin-correlated crystal field, which affects the terms with $S = 1$ only and yields better agreement for $^3K_8$. Yeung and Newman (1986) and Yeung (1987) showed

† Present address: Institut für Physik, Universität Mainz, D-6500 Mainz, Federal Republic of Germany.
‡ Present address: Thyssen Stahl Aktiengesellschaft, POB 11 05 61, D-4100 Duisburg 11, Federal Republic of Germany.

0953-8984/90/214685 + 16 $03.50

for Ho^{3+} in YPO_4, however, that spin correlation leads to an improvement in the theoretical description for the term $^3K_8$, but not for the terms $^5G_{2,5,6}$, possibly because of misidentification of energy levels.

This was the motivation for us to start comprehensive investigations on the spectra of Ho^{3+} in a series of compounds, including the analysis of the crystal-field splittings and their description by improved theoretical models. The studies were based on partly unpublished findings of former members of our group on crystals with the zircon structure, namely on Ho^{3+} in YPO_4 by Becker *et al* (1969), on Ho^{3+} in YVO_4 by Schlaphof (1970) and on Ho^{3+} in $YAsO_4$ by Schwab (1973), respectively. The former results were checked and extended by using magnetic fields in special directions. The analysis was completed, and some terms were assigned for the first time.

The first three publications in this series deal solely with experimental results found on Ho^{3+} in YVO_4 (this paper), in $YAsO_4$ and in $HoPO_4$ (Enderle *et al* 1990a, b), where the latter two will henceforth be denoted as II and III, respectively. Two forthcoming papers are concerned with experimental findings on Ho^{3+} in $Y(OH)_3$ (Pilawa 1990a) and in $LiYF_4$ (Pourat *et al* 1990). In a subsequent, mainly theoretical, paper, the influence of the correlated crystal field (Bishton and Newman 1970) on the splittings of the Ho^{3+} ion in the various substances will be treated (Pilawa 1990b).

2. Experimental details

Single crystals of $(Ho_{0.1},Y_{0.9})VO_4$ were grown by a flux method (Hintzmann and Müller-Vogt 1969). They crystallise in the tetragonal zircon structure $I4_1/amd$, with the point symmetry of the Ho^{3+} sites being $\bar{4}m2$ in the crystallographic *abc* system or $\bar{4}2m$ in an *xyz* system rotated by $\pi/2$ around the $c \equiv z$ axis. The latter is used in the following. The crystals had thicknesses between 0.1 and 2 mm and were irradiated along $\boldsymbol{c}$ or perpendicular to $\boldsymbol{c}$; for the former purpose they were cut and polished perpendicularly to $\boldsymbol{c}$.

Polarised absorption spectra were taken using a 3.4 m Ebert grating spectrograph with a dispersion of about 0.1 nm mm^{-1} and a resolution limited by the 50 μm entrance and exit slits. The spectra were recorded automatically by data processing with a photomultiplier on a step-driven slide.

Measurements were made at temperatures between 1.4 and 85 K in a gas-flow cryostat using liquid ^4He, liquid nitrogen or liquid air. Magnetic fields up to 4 T could be applied by means of a superconducting coil.

The investigations were extended over the spectral range from 11 000 to 27 600 cm^{-1}. The energetic positions of the absorption lines were determined by comparison with emission lines of an iron arc. The selection of 6–10 lines from the respective wavenumber interval of 600 cm^{-1} provided an absolute accuracy of about ± 0.2 cm^{-1}.

3. Theoretical remarks

3.1. Crystal-field states

The free Ho^{3+} ion has the electron configuration $4f^{10}$. Its eigenfunctions can be written in the form $|\gamma JM\rangle$, where J and M are the quantum numbers of the angular momentum operators J^2 and J_z, and γ represents the quantum numbers of all other operators that

commute with J^2 and J_z. Intermediate-coupling eigenfunctions for all terms up to an energy of about 30 000 cm^{-1} have been given by Rajnak and Krupke (1967) and by Domann (1974).

The point symmetry $\bar{4}2m$ of the Ho^{3+} site in $(Ho,Y)VO_4$ is generated by each pair of the following symmetry elements:

(i) a fourfold inversion axis $\bar{4}$ along $\boldsymbol{c}$;
(ii) a twofold rotation axis 2 along $\boldsymbol{x}$ or $\boldsymbol{y}$;
(iii) a mirror plane ac or bc.

If an external field is applied along one of the principal axes, two of the symmetry elements are broken, but one (of course, depending on the field axis chosen) remains unaffected.

The terms of the free ion are split by the crystal field into components, their crystal-field states (eigenfunctions)

$$|j\bar{\mu}\nu S\rangle = \sum_{\gamma JM} a_{j\gamma JM}\,|\gamma JM\rangle \tag{1}$$

being linear combinations of the eigenfunctions of the free ion, where j is a running index. These states are characterised by their behaviour with regard to the symmetry transformations of $\bar{4}2m$. Rotations of the coordinate system by $\pi/2$ around the crystal c axis and inversion gives

$$\bar{4}|j\bar{\mu}(\nu S)\rangle = \exp(i\tfrac{1}{2}\pi\bar{\mu})|j\bar{\mu}(\nu S)\rangle. \tag{2}$$

Singlet states will also satisfy

$$2|j\bar{\mu}\nu S\rangle = \exp(i\pi\nu)|j\bar{\mu}\nu S\rangle \tag{3}$$

for a rotation by π around the y axis and

$$m|j\bar{\mu}\nu S\rangle = (-1)^S|j\bar{\mu}\nu S\rangle \tag{4}$$

for a reflection at the bc plane.

The crystal quantum numbers $\bar{\mu}$, ν and S are restricted to the values $\bar{\mu} = 0, \pm 1, 2$, $\nu = 0, 1$ and $S = 0, 1$. There are four different types of singlet states with $\bar{\mu} = 0, 2$, $\nu = 0, 1$ and $S = 0, 1$, and one type of doublet state with $\bar{\mu} = \pm 1$. Under the operations 2 and m, respectively, the two states of every doublet are transformed into each other, and thus ν and S are not defined. Since the symmetry $\bar{4}2m$ is already generated by each pair of the above symmetry elements, two crystal quantum numbers are sufficient to specify the singlet states; the third one follows from the relation $\bar{\mu}(\mathrm{mod}\,4) = 2(S + \nu)$.

Neglecting configuration interaction in equation (1), all states of the free Ho^{3+} ion have definite, in this case even, parity. Thus a crystal-field state $|j\bar{\mu}\nu S\rangle$ consists of free-ion functions $|\gamma JM\rangle$ with $M = \bar{\mu}(\mathrm{mod}\,4)$. For the singlets the values of ν or S determine whether the M values appear in the symmetric combination $|\gamma J, M\rangle_s = (1/\sqrt{2})(|\gamma J, M\rangle + |\gamma J, -M\rangle)$ or the antisymmetric one $|\gamma J, M\rangle_a = (1/\sqrt{2})(|\gamma J, M\rangle - |\gamma J, -M\rangle)$. The symmetry types of the crystal-field states and their combination of free-ion functions of even parity are presented in table 1, where the abbreviation $|\gamma JM\rangle = |M\rangle$ is used. There the irreducible representations after Koster *et al* (1966) are also included. In the following, a crystal-field state, omitting the running index j, is specified merely by its crystal quantum numbers as $|\bar{\mu}\nu S\rangle$ in the case of a singlet and as $|\pm\bar{\mu}\rangle$ in the case of a doublet.

Table 1. The symmetry properties of the crystal-field states of Ho^{3+} at a site of symmetry $\bar{4}2m$.

	Irreducible representation (Koster)	Crystal quantum number			Basis states $\|(J)M\rangle$† of even parity	
		$\bar{\mu}$	ν	S	for J even	for J odd
Singlet	Γ_1	0	0	0	$\|0\rangle, \|4\rangle_s, \|8\rangle_s$	$\|4\rangle_a, \|8\rangle_a$
	Γ_2	0	1	1	$\|4\rangle_a, \|8\rangle_a$	$\|0\rangle, \|4\rangle_s, \|8\rangle_s$
	Γ_3	2	0	1	$\|2\rangle_s, \|6\rangle_s$	$\|2\rangle_a, \|6\rangle_a$
	Γ_4	2	1	0	$\|2\rangle_a, \|6\rangle_a$	$\|2\rangle_s, \|6\rangle_s$
Doublet	Γ_5	±1	—	—	$\|\pm1\rangle, \|\mp3\rangle, \|\pm5\rangle, \|\mp7\rangle$	

† The states refer to the *xyz* coordinate system.

3.2. *Selection rules*

Electric dipole transitions within the $4f^{10}$ configuration are forbidden by the parity selection rule. They are induced by small contributions of odd-parity configurations to the crystal-field states. Magnetic dipole transitions, on the contrary, are allowed within the $4f^{10}$ configuration.

The transitions between the crystal-field states obey selection rules with respect to $\bar{\mu}$, ν and S, which follow from the transformation behaviour of the electric or magnetic dipole operator, especially under the symmetry operations of the Ho^{3+} site. Without a magnetic field, the *a* and *b* directions or the *x* and *y* directions, respectively, are equiv-

Table 2. Selection rules for optical transitions in a crystal field of point symmetry $\bar{4}2m$. $\boldsymbol{E}$ and $\boldsymbol{H}$ are the electric and magnetic vectors, respectively, of the incident light.

Direction of incident light	Polarisation	Electric dipole transitions	Magnetic dipole transitions
Without magnetic field			
$\boldsymbol{k} \perp \boldsymbol{c}$	σ: $\boldsymbol{E} \perp \boldsymbol{c}, \boldsymbol{H} \parallel \boldsymbol{c}$	$\Delta\bar{\mu} = \pm1 (\mathrm{mod}\ 4)$	$\Delta\bar{\mu} = 0, \Delta\nu = \pm1, \Delta S = \pm1$
	π: $\boldsymbol{E} \parallel \boldsymbol{c}, \boldsymbol{H} \perp \boldsymbol{c}$	$\Delta\bar{\mu} = 2 (\mathrm{mod}\ 4), \Delta\nu = \pm1, \Delta S = 0$	$\Delta\bar{\mu} = \pm1 (\mathrm{mod}\ 4)$
$\boldsymbol{k} \parallel \boldsymbol{c}$	$\sigma(\boldsymbol{k} \parallel \boldsymbol{c})$: $\boldsymbol{E} \perp \boldsymbol{c}, \boldsymbol{H} \perp \boldsymbol{c}$	$\Delta\bar{\mu} = \pm1 (\mathrm{mod}\ 4)$	$\Delta\bar{\mu} = \pm1 (\mathrm{mod}\ 4)$
Magnetic field $\boldsymbol{B} \parallel \boldsymbol{a}$			
$\boldsymbol{k} \parallel \boldsymbol{c}$	a: $\boldsymbol{E} \parallel \boldsymbol{a}, \boldsymbol{H} \parallel \boldsymbol{b}$	$\Delta S = \pm1$	$\Delta S = \pm1$
	b: $\boldsymbol{E} \parallel \boldsymbol{b}, \boldsymbol{H} \parallel \boldsymbol{a}$	$\Delta S = 0$	$\Delta S = 0$
$\boldsymbol{k} \perp \boldsymbol{c}$	σ: $\boldsymbol{E} \parallel \boldsymbol{a}, \boldsymbol{H} \parallel \boldsymbol{c}$	$\Delta S = \pm1$	$\Delta S = \pm1$
	π: $\boldsymbol{E} \parallel \boldsymbol{c}, \boldsymbol{H} \parallel \boldsymbol{a}$	$\Delta S = 0$	$\Delta S = 0$
Magnetic field $\boldsymbol{B} \parallel \boldsymbol{y}$			
$\boldsymbol{k} \parallel \boldsymbol{c}$	x: $\boldsymbol{E} \parallel \boldsymbol{x}, \boldsymbol{H} \parallel \boldsymbol{y}$	$\Delta\nu = \pm1$	$\Delta\nu = 0$
	y: $\boldsymbol{E} \parallel \boldsymbol{y}, \boldsymbol{H} \parallel \boldsymbol{x}$	$\Delta\nu = 0$	$\Delta\nu = \pm1$
Magnetic field $\boldsymbol{B} \parallel \boldsymbol{c}$			
$\boldsymbol{k} \perp \boldsymbol{c}$	σ: $\boldsymbol{E} \perp \boldsymbol{c}, \boldsymbol{H} \parallel \boldsymbol{c}$	$\Delta\bar{\mu} = \pm1 (\mathrm{mod}\ 4)$	$\Delta\bar{\mu} = 0$
	π: $\boldsymbol{E} \parallel \boldsymbol{c}, \boldsymbol{H} \perp \boldsymbol{c}$	$\Delta\bar{\mu} = 2 (\mathrm{mod}\ 4)$	$\Delta\bar{\mu} = \pm1 (\mathrm{mod}\ 4)$
$\boldsymbol{k} \parallel \boldsymbol{c}$[a]	σ_+: $\boldsymbol{E}_+, \boldsymbol{H}_+$	$\Delta\bar{\mu} = -1 (\mathrm{mod}\ 4)$	$\Delta\bar{\mu} = +1 (\mathrm{mod}\ 4)$
	σ_-: $\boldsymbol{E}_-, \boldsymbol{H}_-$	$\Delta\bar{\mu} = +1 (\mathrm{mod}\ 4)$	$\Delta\bar{\mu} = -1 (\mathrm{mod}\ 4)$

[a] The indices + and − refer to right- or left-handed circular polarisation, respectively.

alent, leading to the consequence that the selection rules are the same for any linear polarisation perpendicular to c.

A magnetic field along a breaks all symmetries except that of the mirror plane bc. This leads to the elimination of the selection rules with respect to $\bar{\mu}$ and ν, while the selection rules with respect to S subsist. Thus different selection rules are valid for polarisations parallel and perpendicular to the mirror plane. Similarly, a magnetic field along y suspends the selection rules in $\bar{\mu}$ and S, and different selection rules in ν apply to parallel and perpendicular polarisation with respect to y. In other words, the magnetic field perpendicular to c mixes singlet and doublet states, thus removing the selection rules in $\bar{\mu}$. Table 2 shows the selection rules needed for the analysis of the spectra of Ho^{3+} in YVO_4 and, for the sake of completeness, those which concern Ho^{3+} in $YAsO_4$ and $HoPO_4$ (see parts II and III), too.

Assuming that mixing of terms with different J by the crystal field can be neglected, additional selection rules are effective (Judd 1962, Ofelt 1962):

$$|\Delta J| \leq 6 \qquad \text{for electric dipole transitions} \tag{5}$$

$$|\Delta J| \leq 1 \qquad \text{for magnetic dipole transitions.} \tag{6}$$

Transitions between crystal-field states containing only one particular M value are also restricted by selection rules in M, which are given in table 3.

Table 3. Selection rules with respect to M.

Polarisation	Electric dipole transitions	Magnetic dipole transitions
$\pi\,(\boldsymbol{E} \parallel c, \boldsymbol{H} \perp c)$	$\Delta M = \pm 2, \pm 6$	$\Delta M = 0$
$\sigma\,(\boldsymbol{E} \perp c, \boldsymbol{H} \parallel c)$	$\Delta M = \pm 1, \pm 3, \pm 5$	$\Delta M = \pm 1$
Only with magnetic field $\boldsymbol{B} \parallel c$		
$\sigma_+\,(\boldsymbol{E}_+, \boldsymbol{H}_+)$	$\Delta M = -1, +3, -5$	$\Delta M = +1$
$\sigma_-\,(\boldsymbol{E}_-, \boldsymbol{H}_-)$	$\Delta M = +1, -3, +5$	$\Delta M = -1$

3.3. Zeeman effect

The doublets are split by a field $\boldsymbol{B}_\parallel$ along the c axis. For small fields, the shift is linear and given by

$$E_{j\bar{\mu}}(B_\parallel) = \sum_M |a_{j\bar{\mu}\gamma JM}|^2 Mg\mu_B B_\parallel = s_{j\bar{\mu}}\mu_B B_\parallel \tag{7}$$

where g is the Landé g-factor of the respective term, μ_B is the Bohr magneton and $s_{j\bar{\mu}}$ is the splitting factor of the doublet, which, in a generalised definition, can be written as

$$s_{j\bar{\mu}} = \partial E_{j\bar{\mu}}/\partial(\mu_B B). \tag{8}$$

The sum in equation (7) includes all values of M that, according to table 1, belong to the particular $\bar{\mu}$. For larger fields and in the case in which two doublets are near to each other, an additional shift quadratic in the field can appear. The singlets experience at most a quadratic shift, which, in high fields and with small distance of neighbouring singlets with the same value of M, can go over into a linear effect. This case is also

Table 4. Energies, crystal quantum numbers and Zeeman splitting factors.

J term	Centre of gravity (cm^{-1})	Energy of the component (cm^{-1})	Crystal quantum numbers $\bar{\mu}$	ν	S	Splitting factor
$^5I_8$		0.0	0	0	0	
		20.7	±1			
		46.5	±1			
		46.5	2	1	0	
		116.6	2	0	1	
		132.0	2	1	0	
$^5I_5$	11 242.7	11 211.6	±1			
		11 213.1	2	0	1	
		11 226.9	0	1	1	
		11 241.8	±1			
		11 243.6	2	1	0	
		11 259.0	±1			
		11 271.1	0	0	0	
		11 290.5	0	1	1	
$^5F_5$	15 462.6	15 401.1	±1			2.6
		15 410.9	2	0	1	
		15 414.7	0	1	1	
		15 438.0	±1			2.9
		15 486.0	0	0	0	
		15 519.4	2	1	0	
		15 523.2	±1			−1.4
		15 532.7	0	1	1	
$^5S_2$	18 396.7	18 386.9 ± 0.7[a]	2	0	1	
		18 394.1	0	0	0	
		18 394.7	±1			1.46
		18 413.1	2	1	0	
$^5F_4$	18 525.7	18 486.4	±1			−3.51
		18 498.4	0	0	0	
		18 518.8	0	1	1	
		18 535.5	0	0	0	
		18 538.1	±1			1.12
		18 557.9	2	0	1	
		18 571.4	2	1	0	
$^5F_3$	20 578.8	20 520.0	2	1	0	
		20 537.9	±1			−0.95
		20 600.6	±1			−1.71
		20 620.2 ± 1.0[a]	2	0	1	
		20 634.1 ± 0.6[a]	0	1	1	
$^5F_2$	21 038.1	20 988.0 ± 3.4[a]	2	0	1	
		21 030.5	±1			0.91
		21 059.0	0	0	0	
		21 082.3	2	1	0	
$^3K_8$	21 352.4	21 295.2	0	0	0	−4.6
		21 302.4	0	1	1	
		21 315.6	±1			−3.06
		21 319.0 ± 5.5[b]	0	0	0	
		21 319.0 ± 5.5[b]	0	1	1	

Table 4. (*contd*)

J term	Centre of gravity (cm^{-1})	Energy of the component (cm^{-1})	Crystal quantum numbers			Splitting factor
			$\bar{\mu}$	ν	S	
		21 323.2	±1			4.51
		21 342.1	2	0	1	
		21 361.1	2	1	0	
		21 362.0	2	0	1	
		21 382.5	2	1	0	
		21 401.6	±1			1.28
		21 407.4	±1			−7.74
		21 411.3	0	0	0	
$^5G_6$	22 055.2	21 924.2	0	0	0	
		21 927.4	±1			3.0
		21 970.2	2	0	1	
		22 012.0	±1			1.4
		22 018.8	0	1	1	
		22 092.2	2	1	0	
		22 130.4	2	0	1	
		22 164.8	0	0	0	
		22 165.3	±1			−1.6 to 0.0[b]
		22 207.7	2	1	0	
$^5F_1$	22 260.3	22 251.7	0	1	1	
		22 264.6	±1			0
$^5G_5$	23 902.2	23 828.2	2	1	0	
		23 833.1	±1			−2.2
		23 848.9	0	1	1	
		23 889.3	0	0	0	
		23 896.0	±1			5.6
		23 959.1	2	0	1	
		23 974.1	±1			≈0
		23 991.9 ±1.2[a]	0	1	1	
$^5G_4$	25 767.9	25 712.4	2	0	1	
		25 719.9	2	1	0	
		25 746.0	0	0	0	
		25 751.5	0	1	1	
		25 767.9	±1			1.09
		25 811.2	±1			−3.44
		25 823.1	0	0	0	
$^3K_7$	26 130.0	26 113.8	0	1	1	−3.9
		26 113.8	0	0	0	
		26 114.8	±1			−3.0
		26 121.4	±1			−7.0
		26 121.4	2	1	0	
		26 124.5	±1			5.0
		26 130.6	2	0	1	
		26 144.6	±1			1.0
		26 152.2	2	1	0	
		26 152.2	2	0	1	
		26 154.5	0	1	1	
$^3H_5$	27 522.5	27 471.0	±1			1.3
		27 476.0	0	1	1	

Table 4. (*contd*)

J term	Centre of gravity (cm^{-1})	Energy of the component (cm^{-1})	Crystal quantum numbers $\bar{\mu}$	ν	S	Splitting factor
		27 479.3	2	0	1	
		27 516.3	2	1	0	
		27 532.3	±1			−1.6
		27 538.3	0	0	0	
		27 571.3	0	1	1	
		27 579.6	±1			4.9

[a] Determined from measurements with perpendicular fields.
[b] See text.

described by a splitting factor according to equation (8). The splitting factors of the doublets quoted in table 4 are calculated for $B_{\parallel} = 0$, those of the singlets for $B_{\parallel} = 3$ T.

Fields perpendicular to the *c* axis generally cause quadratic shifts of both doublets and singlets.

4. Procedure of the analysis

As is common practice, linearly polarised spectra were taken at various temperatures in order to determine the energies and the symmetry types of the low-lying components of the ground term $^5I_8$ and the components of the excited terms.

The lowest ground-term component of Ho^{3+} in YVO_4 is a singlet state $|000\rangle$ (in contrast to Ho^{3+} in $YAsO_4$ and YPO_4, where it is a doublet in both cases). This gives some complications in the analysis. At low temperatures, where only the lowest component $|000\rangle$ is populated, transitions in electric dipole radiation are allowed only to the doublets and the singlets $|210\rangle$ of the excited terms. Thus, using merely low temperatures, the analysis will remain incomplete. The normal escape route is to use higher temperatures, to be able to observe transitions from excited components of the ground term. The disadvantage is that, with increasing temperature, the number of absorption lines increases and with that the possibility of overlapping. Furthermore, not all of the allowed transitions are actually observed because of low transition probabilities.

Additional to this method, we developed an alternative approach avoiding the use of elevated temperatures. A magnetic field applied along ***a*** or ***y*** induces (primarily forbidden) transitions from the ground-term singlet $|000\rangle$ to the singlets of the excited terms with growing intensity for increasing field strength. From the polarisation of these transitions (parallel to ***a*** or ***b*** and to ***x*** or ***y***, respectively; see table 2), the crystal quantum numbers S and ν, respectively, of the individual singlet can be determined. The energies of the transitions are, to a first approximation, shifted proportional to the square of the field strength. Thus the energy of the respective singlet can be ascertained by backward extrapolation of the measured energies using the optimised parabola with zero slope at zero field. The square root of the mean-square difference σ between the experimental points and the best parabola was used to estimate the error bars of the energy. The upper and the lower parabolae resulting in a deviation 2σ were calculated and half of their energy difference at $B = 0$ was taken as the uncertainty.

The splittings (with $\boldsymbol{B} \parallel \boldsymbol{c}$) of the doublets were determined from the spectra taken in the field range 0 to 4 T in steps of 0.5 or 1 T (in some cases also in steps of 0.2 or 0.25 T in the range up to 1 T). For a first estimate, a linear and symmetric shift of the doublet components was assumed given by the mean straight line through the measuring points. The sign of the splitting factors was chosen so as to result in a g-factor as close as possible to the theoretical free-ion value for the term in question. The splitting factors thus obtained were checked by a simple calculation with the doublets alone. The crystal-field matrix elements and the g-factor for the term required for this calculation are already determined by the energy distances of the doublets at zero field and their splitting factors. In that manner it could be tested rather easily whether or not the measurements and the calculations were consistent. A rather good agreement resulted for most of the terms. No adjustment of measured and calculated Zeeman energies could be found for the terms $^5F_5$, $^5G_6$ and $^3H_5$, even if the splitting factors were varied. This indicates that influences of J mixing may be especially effective in these cases.

5. Experimental results

5.1. Tabular summary of the findings

The results of former studies of members of our group (Schlaphof 1970, Laugsch 1971) and of our latest investigations are comprehensively collected in table 4. The energies are related to the lowest component of the ground term $^5I_8$. The errors of the energies normally are $\pm 0.2\ cm^{-1}$; larger errors are given in the table

5.2. Discussion of the individual terms

In the following, some characteristics and peculiarities are described that appeared in the analysis of the individual terms. Unequivocal results regarding energy, crystal quantum numbers and splitting factor are not mentioned.

5.2.1. $^5I_8$. Six of the 13 crystal-field components of this term were found. The symmetry type of the lowest singlet $|000\rangle$ was determined by Laugsch (1971) using a field perpendicular to $\boldsymbol{c}$. The Zeeman effect of the four lowest-lying components is given in Bleaney *et al* (1988). It turns out that the lowest singlet $|000\rangle$ mainly consists of the $|M = 0\rangle$ state ($|000\rangle = -0.948|M = 0\rangle + 0.320|M = \pm 4\rangle_s + 0.006|M = \pm 8\rangle_s$); the first excited doublet is an almost pure $|M = \pm 1\rangle$ and the next doublet an $|M = \pm 7\rangle$.

5.2.2. $^5I_5$. All components were assigned from measurements at various temperatures. The lines are not very sharp. Both singlets $|011\rangle$ and the singlet $|201\rangle$ are excited from the two low-lying doublets, but obviously not from singlets, which would be necessary to determine the symmetry types with certainty. This term was not investigated in perpendicular fields.

5.2.3. $^5F_5$. Within this term, the sharpness of the lines decreases with increasing wavenumber. All components were determined by measurements at different temperatures. The position of the singlet $|201\rangle$ is not very certain since the respective transitions are weak and the singlet could not be observed in perpendicular fields. It was not possible to reproduce the measured Zeeman energies by calculations as described in section

4 although the signs of the splitting factors were confirmed by circularly polarised measurements with $\boldsymbol{k} \parallel \boldsymbol{c}$.

5.2.4. $^5S_2$. The component $|201\rangle$ could only be determined by means of perpendicular fields. Its energy at zero field was deduced from the energies at 1 T and 4 T for $\boldsymbol{B} \parallel \boldsymbol{a}$. The uncertainty in energy given in table 4 is estimated using $\sigma = 0.2$ (as found in other cases).

5.2.5. $^5F_4$. In addition to the determination from higher temperatures, all components were observed in perpendicular fields with the exception of $|011\rangle$. The symmetry type of this singlet was assured by the corresponding transition of Ho^{3+} in $TbVO_4$, which is allowed in the Jahn–Teller-distorted phase with the reduced point symmetry 222.

5.2.6. $^5F_3$. The singlets $|011\rangle$ and $|201\rangle$ could not be excited directly from any ground-term component up to 132 cm^{-1}. In perpendicular fields $\boldsymbol{B} \parallel \boldsymbol{y}$ and $\boldsymbol{B} \parallel \boldsymbol{a}$, transitions from the ground singlet $|000\rangle$ to these singlets were observed. Figure 1 shows the spectrum for the term at $B = 4$ T and $T = 1.4$ K. The energies at $B = 0$ were calculated using measurements from 1 to 4 T in steps of 0.5 T.

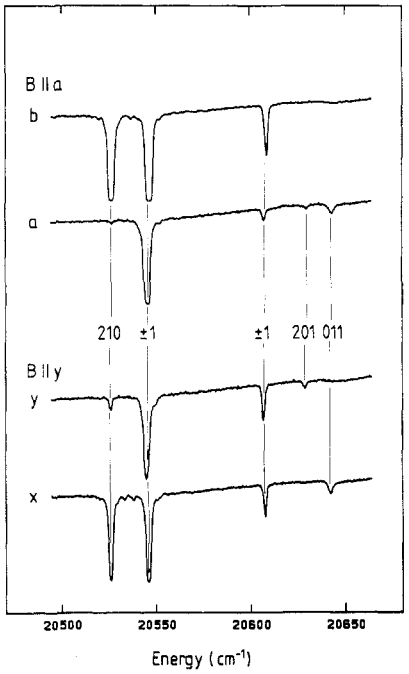

Figure 1. Transitions to the term $^5F_3$ at $B = 4$ T, $T = 1.4$ K with $\boldsymbol{B} \parallel \boldsymbol{a}$, $\boldsymbol{E} \parallel \boldsymbol{b}$ or $\boldsymbol{E} \parallel \boldsymbol{a}$ and $\boldsymbol{B} \parallel \boldsymbol{y}$, $\boldsymbol{E} \parallel \boldsymbol{y}$ or $\boldsymbol{E} \parallel \boldsymbol{x}$, respectively. The labels are the crystal quantum numbers $\bar{\mu}$, ν and S of the components of $^5F_3$.

5.2.7. $^5F_2$. At 1.4 K an unusual step was observed in the recorded σ spectrum below the transition $|000\rangle \rightarrow |\pm 1\rangle$. At 20 K neither this step nor another line corresponding to the transitions from the excited ground-term doublets to the singlet $|201\rangle$ was found. In perpendicular fields, a weak line was observed in the range of the step, which, according to its polarisation, was attributed to the transition $|000\rangle \rightarrow |201\rangle$. The zero-field energy of $|201\rangle$ was calculated using the energies of all components of this term at 4 T for $\boldsymbol{B} \parallel \boldsymbol{a}$ and $\boldsymbol{B} \parallel \boldsymbol{y}$ and the zero-field energies of the components except $|201\rangle$ under the

assumption that the centre of gravity of the $S = 1$ states and that of the $S = 0$ states are independent of the field strength for $\boldsymbol{B} \parallel \boldsymbol{a}$ and the corresponding assumption for the $v = 0$ ($v = 1$) states for $\boldsymbol{B} \parallel \boldsymbol{y}$. Since these conditions may not be strictly valid, the energy of $|201\rangle$ is given only within $\pm 3.4\ \mathrm{cm}^{-1}$.

5.2.8. $^3K_8$. All components except the singlets at about $21\,319\ \mathrm{cm}^{-1}$ were assigned from measurements at high temperatures. In addition, the quantum number S could be proved in fields along $\boldsymbol{a}$. The transitions are very sharp with linewidths of $5\ \mathrm{cm}^{-1}$ and less. The four doublets form two pairs separated by about $75\ \mathrm{cm}^{-1}$. The measured Zeeman splittings are consistent with the assumption of rather pure M states. The doublet with the splitting factor 1.28 is excited from the ground singlet $|000\rangle$ not only by electric but also by magnetic dipole radiation in accordance with the selection rules in J (equation (6)) and M (table 3). The singlets of types $|201\rangle$ and $|210\rangle$ form a distinct arrangement: the quasi-degenerate pair $|201\rangle$–$|210\rangle$ with mainly $M = \pm 6$ (from measurements and comparing calculations with $\boldsymbol{B} \parallel \boldsymbol{a}$) is framed by the singlets $|201\rangle$ and $|210\rangle$ with mainly $M = \pm 2$, their respective centres of gravity being nearly the same. A $|000\rangle$–$|011\rangle$ pair with mainly $M = \pm 4$ (from measurements with $\boldsymbol{B} \parallel \boldsymbol{c}$) is formed by the singlets with lowest energies. The $|011\rangle$ (and with $\boldsymbol{B} \parallel \boldsymbol{c}$ the $|000\rangle$, too) is excited also by magnetic dipole radiation (due to the $M = \pm 4$ contributions to the ground singlet $|000\rangle$). With a field of 4 T along $\boldsymbol{a}$, a fifth line appears in the range of the lower pair of doublets. Since the line is unpolarised, a second $|000\rangle$–$|011\rangle$ pair is suggested in this region. It should mainly contain $M = \pm 8$. The uppermost singlet $|000\rangle$ is supposed to be an almost pure $|M = 0\rangle$ (as is observed in $YAsO_4$ and YPO_4, too; see parts II and III).

5.2.9. $^5G_6$. This term shows a remarkably large crystal-field splitting ($\sim 280\ \mathrm{cm}^{-1}$). The spectrum observed at 1.4 K is reproduced in figure 2(*a*). The transition from $|000\rangle$ to the uppermost doublet is extremely broad and has a large intensity, which is reduced with increasing temperature, so that further transitions could be established in its surrounding (figure 2(*c*)). The splitting factor of this doublet is uncertain. Figure 2(*b*) shows the spectrum with a field along $\boldsymbol{a}$. Strongly polarised transitions from the ground singlet to the singlets below $22\,100\ \mathrm{cm}^{-1}$ were observed. Their estimated zero-field energies were utilised to decompose the spectra measured at various temperatures without the external field. An analysis of the spectrum at 34 K is given in figure 2(*c*). Both singlets $|000\rangle$ were excited from the singlet $|210\rangle$ at $132\ \mathrm{cm}^{-1}$, the $|011\rangle$ from the $|201\rangle$ at $116.6\ \mathrm{cm}^{-1}$, which are transitions suitable to specify the symmetry types of the excited singlets. The lower singlet $|201\rangle$ was only excited from the $|\pm 1\rangle$ at $20.7\ \mathrm{cm}^{-1}$, the lower $|210\rangle$ from both ground-term doublets. After all transitions to the doublets, to the upper $|000\rangle$ and to singlets found with $\boldsymbol{B} \parallel \boldsymbol{a}$ were assigned, two σ-polarised lines remained, which were attached to the transitions from the first excited ground-term doublet to the upper singlets $|201\rangle$ and $|210\rangle$, respectively. This assignment is not in contradiction to the measurements with perpendicular field. The measured Zeeman splittings cannot be reproduced by calculation (see section 4) although the sign of the splitting factors was confirmed by circularly polarised spectra with $\boldsymbol{k} \parallel \boldsymbol{c}$.

5.2.10. $^5F_1$. The spectra of this term are shown together with the $^5G_6$ in figures 2(*a*)–(*c*). According to the selection rule $|\Delta J| \leq 6$ (equation (5)), the transitions $^5I_8 \rightarrow {}^5F_1$ should not be allowed, unless other terms are mixed into the terms $^5F_1$ and/or $^5I_8$ by the crystal field. The transitions to the doublet state are quite intense and, additionally, two very weak transitions to the $|011\rangle$ from the first doublet and the $|201\rangle$ of the ground term,

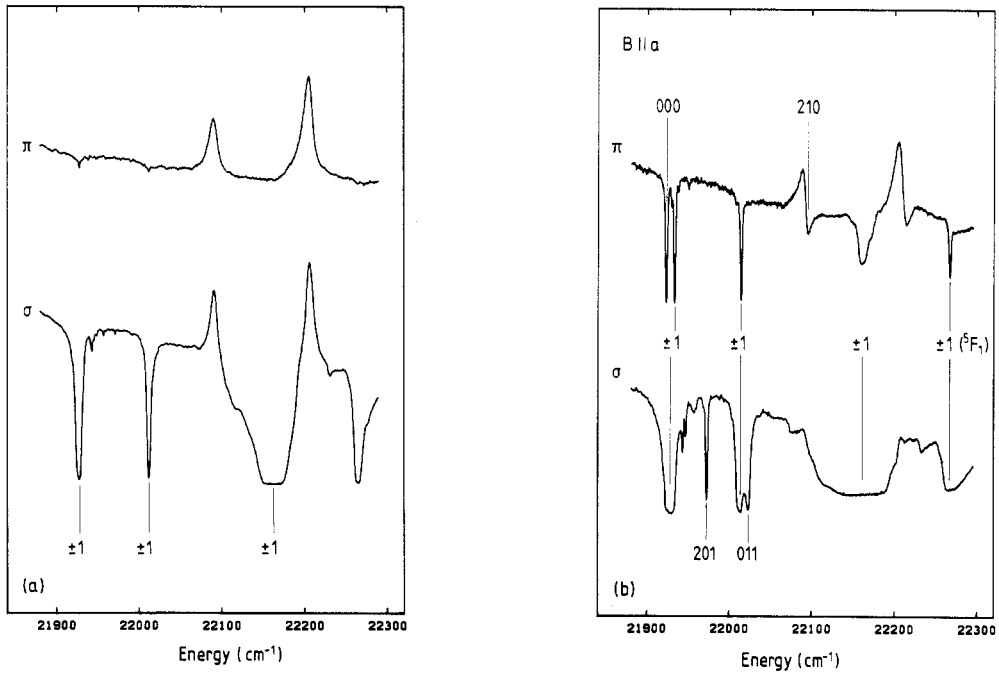

Figure 2. Transitions to the terms $^5G_6$ and $^5F_1$. (*a*) $B = 0$, $T = 1.4$ K. The π-polarised spectrum shows (apart from weak depolarisations of the transitions to the doublets) no Ho^{3+} transitions but two emission lines of the Xe lamp used, which appear in all spectra of this region. (*b*) $\boldsymbol{B} \parallel \boldsymbol{a}$, $B =$ 2 T, $T = 1.4$ K. The spectra with $\boldsymbol{k} \parallel \boldsymbol{b}$ are taken on a thicker crystal than in (*a*) and (*c*). (*c*) $B = 0$, $T =$ 34 K. The transitions from all lower components of $^5I_8$ to each component of $^5G_6$ or $^5F_1$ are collected by one horizontal line, which is labelled with the crystal quantum numbers of the respective component of $^5G_6$ or $^5F_1$. The full circles mark the energies of the possible (not necessarily allowed) transitions from the respective components of $^5I_8$. The quantum numbers of these components are given only once at the top line on the left side. An observed absorption that corresponds to an allowed transition is connected to the horizontal line by a vertical line. A short line indicates an allowed but not observed transition and a full circle without a vertical line indicates a forbidden transition. The singlet states of $^5G_6$ are assigned above and the doublet states below the spectra and the states of $^5F_1$ between the spectra. A small part of the π spectrum at 50 K is included because the additional absorption line ascertains energy and symmetry type of the upper singlet $|000\rangle$.

respectively, were found. Some further weak absorptions observed with $\boldsymbol{B} \parallel \boldsymbol{a}$ do not agree with the energy 22 251.7 cm^{-1} of the $|011\rangle$ and may have another origin.

5.2.11. $^5G_5$. In the low-energy region of this term, numerous satellite lines are observed, especially at low temperatures. The upper $|011\rangle$ was not excited from the two ground-term doublets, not even at higher temperature. It could be observed, however, at 1.4 K at a field of 4 T along $\boldsymbol{a}$ and fields above 1.5 T along $\boldsymbol{y}$ with the expected polarisation. Its energy at $B = 0$ was evaluated from the measurements with $\boldsymbol{B} \parallel \boldsymbol{y}$ in the range 1.5 to 4 T (in steps of 0.5 T). The transition $|000\rangle \rightarrow |201\rangle$ also appeared in fields along $\boldsymbol{a}$ and $\boldsymbol{y}$ in the correct polarisation. Additionally, the transition from the doublet at 46.5 cm^{-1} to $|201\rangle$ was observed at temperatures above 50 K. The energy of the $|201\rangle$, given in table 4, was derived from the latter transition. The measured doublet splitting factors lead to a rather good agreement with calculations, as described in section 4.

5.2.12. $^5G_4$. All components were assigned from measurements at different temperatures. They could also be derived from investigations at 1.4 K with perpendicular fields, where the upper $|000\rangle$ only appeared at a field of 4 T along $\boldsymbol{a}$. The measured splitting factors result in a good agreement between calculated and measured Zeeman energies.

5.2.13. $^3K_7$. The crystal-field splitting of this term is extremely small (41 cm^{-1}) and the transitions are very sharp (5 cm^{-1} and less). Figure 3(*a*) shows the Zeeman effect for $\boldsymbol{B} \parallel \boldsymbol{c}$. For increasing fields, the doublets partially merge, whereby the eigenfunctions are mixed and/or exchanged. The approximate crossing of components with the same $\bar{\mu}$

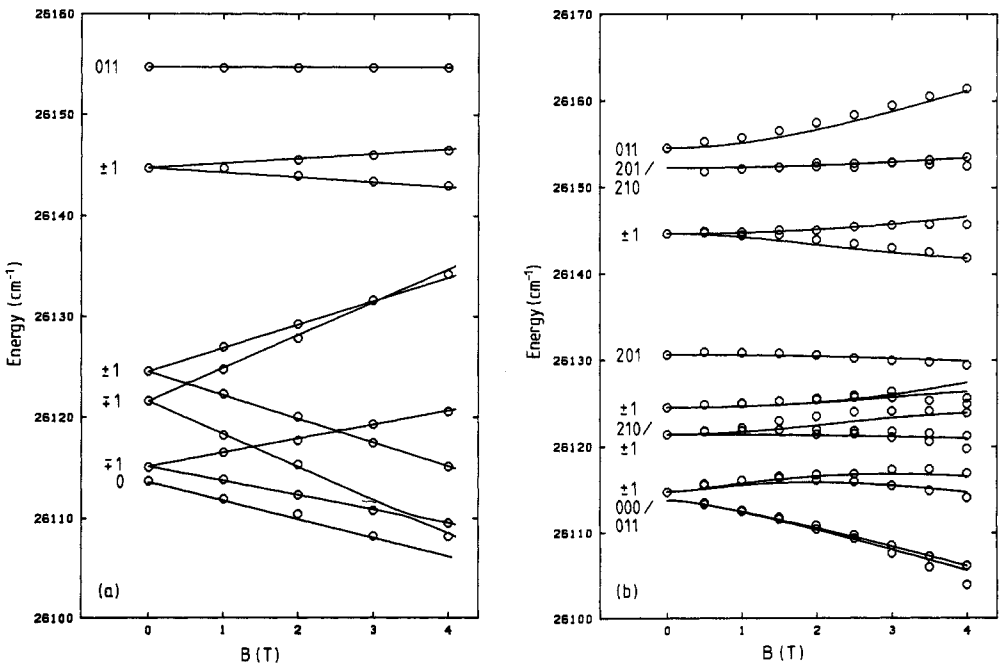

Figure 3. Comparison of measured (open circles) and calculated (full curves) Zeeman effects of the term $^3K_7$ at $T = 1.4$ K. (*a*) $\boldsymbol{B} \parallel \boldsymbol{c}$, (*b*) $\boldsymbol{B} \parallel \boldsymbol{a}$.

indicates that all four doublets are almost pure $|\pm M\rangle$ states. In accordance with the selection rules in J and M, only the doublet with splitting factor 1.0 can be excited by magnetic dipole radiation. Both singlets $|011\rangle$ were observed as magnetic dipole transitions from $|000\rangle$, the upper one (mainly $M = 0$) with medium intensity, the lower one with weak intensity, which rapidly decreased with increasing field along $\boldsymbol{c}$. This fact and the measured splitting factor of -3.9 for the linear shift in high fields indicate that the lower $|011\rangle$ is changed by the field to a predominantly $|M = -4\rangle$. From this a singlet $|000\rangle$ (with mainly $M = +4$ in high fields along $\boldsymbol{c}$) is expected at a slightly higher energy. Figure 3(b) shows the investigation of the Zeeman effect with $\boldsymbol{B} \parallel \boldsymbol{a}$ and $\boldsymbol{k} \parallel \boldsymbol{c}$. The transition to the $|011\rangle$ seemed to appear in the wrong polarisation, probably due to the neighbouring transition to the $|000\rangle$, which showed considerable intensity in this polarisation. For $\boldsymbol{k} \perp \boldsymbol{c}$ both transitions had the correct polarisation. The remaining singlets were determined from measurements with $\boldsymbol{B} \parallel \boldsymbol{a}$ at 1.4 K only. The transition from the $|000\rangle$ to the lower $|201\rangle$ appeared with considerable intensity even in small fields, while the transitions to the upper $|201\rangle$–$|210\rangle$ pair were very weak. A hint of one of the latter singlets was also found at higher temperatures. The lower $|210\rangle$ could hardly be separated from the two inner doublets by means of magnetic fields, but it was detected at higher temperatures. The measured Zeeman effects with $\boldsymbol{B} \parallel \boldsymbol{c}$ and $\boldsymbol{B} \parallel \boldsymbol{a}$ were consistent with calculations based on really pure M states, especially $|M = \pm 6\rangle$ for the upper $|201\rangle$–$|210\rangle$ singlet pair and $|M = \pm 2\rangle$ for the lower $|201\rangle$–$|210\rangle$ pair. These calculations are reproduced by the lines in figures 3(a) and (b).

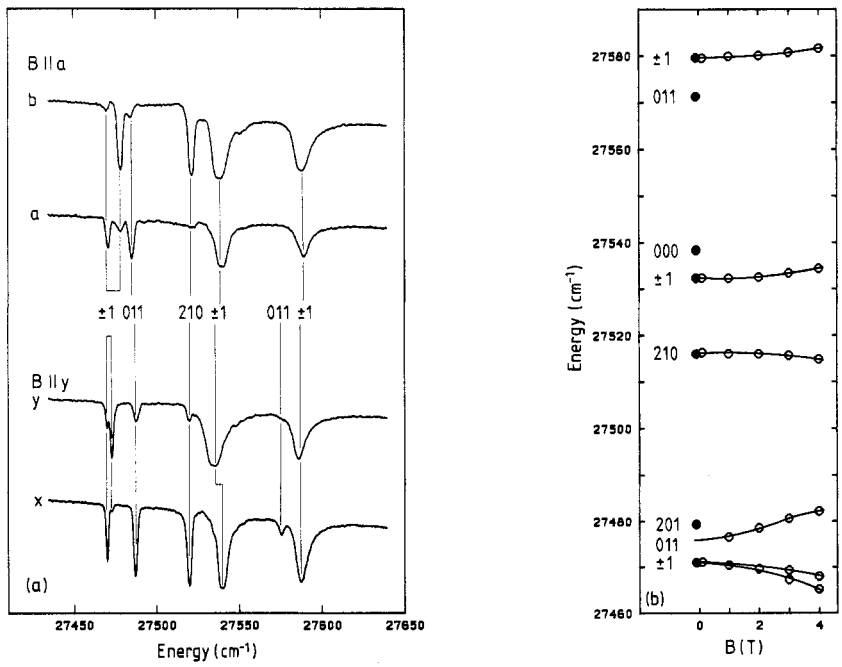

Figure 4. (a) Transitions to the term $^3H_5$ at $B = 4$ T, $T = 1.4$ K. (b) Zeeman effect of the term $^3H_5$ with $\boldsymbol{B} \parallel \boldsymbol{y}$ at 1.4 K (open circles) and zero-field energies at 10 K (full circles). The curves are merely to guide the eye.

5.2.14. $^3H_5$. The spectra with perpendicular fields at 1.4 K are shown in figure 4(*a*). Figure 4(*b*) shows the Zeeman effect with $\boldsymbol{B} \parallel y$ at 1.4 K (open circles), and additionally the energies of the components at 10 K, $B = 0$ (full circles). The energies of all components except the lower $|011\rangle$ were determined from measurements at 10 K without the magnetic field. The studies with perpendicular fields yielded the symmetry types of the singlets with the exception of $|201\rangle$, where a transition could not be induced. Its symmetry type followed from the assignment of all the other singlets. The lower $|011\rangle$ could be found only in perpendicular fields and its energy was determined using four field values between 1 and 4 T. The singlet $|011\rangle$ obviously does not have the energy given by the 10 K transition ($|\pm 1\rangle \rightarrow$ singlet), which consequently was assigned to the singlet $|201\rangle$ (not excited in perpendicular fields). The doublet splitting factors cannot be verified by calculations in the way mentioned in section 4; the sign of the splitting factors was confirmed by circularly polarised measurements with $\boldsymbol{k} \parallel \boldsymbol{c}$.

5.2.15. $^3H_6$. The lines observed at energies above the term $^3H_5$ are very broad and have strange lineshapes. They were not assigned.

6. Conclusions

The spectrum of Ho^{3+} in $(Ho,Y)VO_4$ and its Zeeman effect were investigated in the near-infrared and the entire visible region. At low temperatures and without the field, it consists of a considerably lower number of lines than the spectrum of other substances with the same symmetry of the Ho^{3+} sites. This is due to the fact that the lowest ground-term component of Ho^{3+} in this compound is a singlet, with the consequence that some of the transitions from this component to the crystal-field states of the excited terms are forbidden.

This could be overcome by measurements at different temperatures and by investigations in magnetic fields perpendicular to the crystal *c* axis at low temperatures, by which most of the forbidden transitions were induced.

Combining all these methods, it was possible to analyse the spectrum completely and to determine the energies and the symmetry types of nearly all crystal-field components with great accuracy and certainty.

This paper is solely concerned with a thorough presentation of the experimental results. A discussion of these results and the implications for the validity of the standard models for handling crystal-field interactions will be given by one of us in a subsequent paper (Pilawa 1990).

References

Becker P J 1970 *Phys. Status Solidi* **38** 379–84
—— 1971 *Phys. Status Solidi* b **43** 583–90
Becker P J, Kahle H G and Kuse D 1969 *Phys. Status Solidi* **36** 695–704
Bishton S S and Newman D J 1970 *J. Phys. C: Solid State Phys.* **3** 1753–61
Bleaney B, Gregg J F, Hansen P, Huan C H A, Lazzouni M, Leask M J M, Morris I D and Wells M R 1988 *Proc. R. Soc.* A **416** 63–73
Crosswhite H M, Crosswhite H, Edelstein N and Rajnak K 1977 *J. Chem. Phys.* **67** 3002–10
Domann G 1974 *Diplomarbeit* Universität Karlsruhe
Enderle M, Pilawa B and Kahle H G 1990a *J. Phys.: Condens. Matter* **2** 4711

Enderle M, Pilawa B, Schwab M and Kahle H G 1990b *J. Phys.: Condens. Matter* **2** 4701
Grohmann I, Hellwege K H and Kahle H G 1961 *Z. Phys.* **164** 243–56
Hintzmann W and Müller-Vogt G 1969 *J. Crystal Crowth* **5** 274–8
Hüfner S 1962 *Z. Phys.* **169** 417–26
Judd B R 1962 *Phys. Rev.* **127** 750–61
—— 1977 *Phys. Rev. Lett.* **39** 242–4
Kahle H G 1956 *Z. Phys.* **145** 347–60
Koster G F, Dimmock J O, Wheeler R G and Statz K 1966 *Properties of the Thirty-two Point Groups* (Cambridge, MA: MIT Press)
Laugsch J 1971 *Diplomarbeit* Universität Karlsruhe
Ofelt G S 1962 *J. Chem. Phys.* **37** 511–20
Pilawa B 1990a *J. Phys.: Condens. Matter* at press
—— 1990b to be published
Pourat B, Pilawa B and Kahle H G 1990 to be published
Rajnak K and Krupke W F 1967 *J. Chem. Phys.* **46** 3532–41
Schlaphof W 1970 *Diplomarbeit* Universität Karlsruhe
Schwab M 1973 *Diplomarbeit* Universität Karlsruhe
Yeung Y Y 1987 private communication
Yeung Y Y and Newman D J 1986 *J. Phys. C: Solid State Phys.* **19** 3887–84